Fracture Mechanics of Concrete Structures
Proceedings FRAMCOS-3
AEDIFICATIO Publishers, D-79104 Freiburg, Germany

DELAMINATION CRITERION FOR CONCRETE BEAMS RETROFITTED WITH FRP LAMINATES

O. Buyukozturk, C. Leung, B. Hearing, and O. Gunes
Department of Civil and Environmental Engineering
Massachusetts Institute of Technology
United States

Abstract

The application of fiber-reinforced plastics (FRP) to aging concrete infrastructure has become an attractive choice of structural rehabilitation and retrofit methods worldwide. The load capacity and stiffness of concrete girders can be enhanced by the application of FRP sheets to the tension face of the element, but failures of these systems may become more brittle and can involve debonding failures, generally occurring in the concrete substrate. The debonding mechanism is a local failure process driven by stress intensities associated with stress transfer between the concrete and the laminate. This study examines influences of various design and existing damage parameters on debonding failure modes of the composite system and investigates a quantitative criterion governing these failures. Physical models of reinforced concrete beams are retrofitted with high-strength carbon fiber reinforced plastic sheets and tested in an experimental program. The addition of the FRP is shown to increase the ultimate failure load of the beams, but the specimens are observed to fail through debonding of the retrofitted sheets in the concrete substrate. Influences on static debonding failure mechanisms are investigated, and a quantitative criterion governing delamination is explored through a fracture-energy based analytical procedure.

Key Words: FRP Composite Laminate, Retrofit, Damage, Cracking, Concrete.

1 Introduction

High-strength fiber-reinforced plastics (FRP) offer great potential for lightweight, cost-effective retrofitting of concrete infrastructure through external bonding to concrete members to increase load capacity and stiffnesses. Fiber reinforced plastics have been used to retrofit concrete members such as columns, slabs, beams, and girders in structures including bridges, parking decks, smoke stacks, and buildings. The application of FRP as external reinforcement to concrete structures has been studied by many groups. Theoretical gains in flexural strength using this method can be significant; however, researchers have also observed new types of failures that can limit these gains. These failures are often brittle, involving delamination of the FRP, debonding of concrete layers, and shear collapse, and can occur at loads significatly lower than the theoretical strength of the retrofit system. Among these failure modes, debonding or peeling of the FRP from the concrete surface is a major concern, yet little is known about the fracture processes and characteristics of these mechanisms. Thus, there is a need for improved knowledge of the delamination and peeling failure processes. This paper investigates delamination failures of retrofitted reinforced concrete beams through experimental and analytical studies on laboratory beam specimens retrofitted with FRP laminate. First, available information on delamination failures of FRP retrofitted concrete systems are reviewed. Then, an experimental program conducted to further investigate the local delamination process using initially notched laboratory specimens is presented. Finally, criteria governing the local debonding process are examined, and the application of an energy-based failure criterion for these systems is explored.

2 Failure of Retrofitted Beams by Delamination

FRP retrofitted reinforced concrete has been observed to fail through a variety of modes, which can be grouped into distinct categories such as flexural failures, shear failures, and debonding failures (Buyukozturk and Hearing, 98). Debonding can occur through failure of any constituent material in the system, but the most common debonding mode may be delamination failure of the laminate, adherent, and a thin layer of concrete substrate peeling off of the concrete structure. Delamination failures have been reported in actual rehabilitated structures (Karbhari et al., 97), as well as in research programs incorporating slabs, beams, joints, and

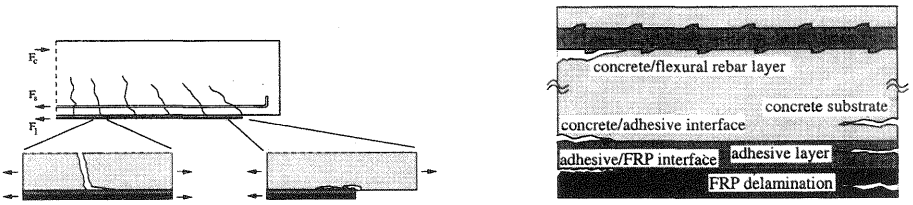

(a) Local stress intensities (b) Possible microcrack locations

Fig. 1. Local stress intensities and microcrack initiation scenarios

columns (Meier, 1992). For these reasons, interest in delamination processes, criteria, and characterization methodologies has increased.

Delamination can be caused by a number of reasons, including relative displacements of concrete in the vicinity of existing cracks, imperfect bonding between the composite and the concrete, cyclic loading induced debonding, environmental degradation, and other application and design specific flaws. Among these causes, delamination initiating from existing cracks or the end of the laminate has been concluded to be highly influential in retrofitted beam members (Meier, 1992). These failure processes are caused by local stress intensities in the concrete beam-adhesive-laminate interfacial region, as illustrated in Fig. 1(a) (Hankers 1997; Taljsten, 1997). These intensities can initiate microcracking in the system at early load levels. Microcracks can form in any of the constituent materials or their interfaces, such as the laminate/adhesive interface, the adhesive/concrete interface, or the concrete/flexural steel layer, as shown in Fig. 1(b). Upon further loading these microcracks propagate and coalesce, ultimately forming macrocracks that can result in system failure.

A variety of simplified models have been used to isolate the peeling failure process and study the bonding interaction between the concrete surface and external reinforcement. Studies have included lap shear pull-off tests (Hankers, 1997), theoretical models of unreinforced open sandwich specimens (Aanandarajah and Vardy, 1985) and peel tests (Karbhari 1997) where local fracture under varying external peel loadings was studied through inclined lap-type specimens. However, the application of this knowledge to laminated reinforced concrete flexural members is limited; the conditions of the concrete substrate in these studies may not have developed the complete microcrack initiation and propagation process found in components with conventional reinforcement subjected to generalized flexure and shear loadings. Thus, there exists a need for isolated study of local delamination mechanisms of reinforced members under flexural beam loading.

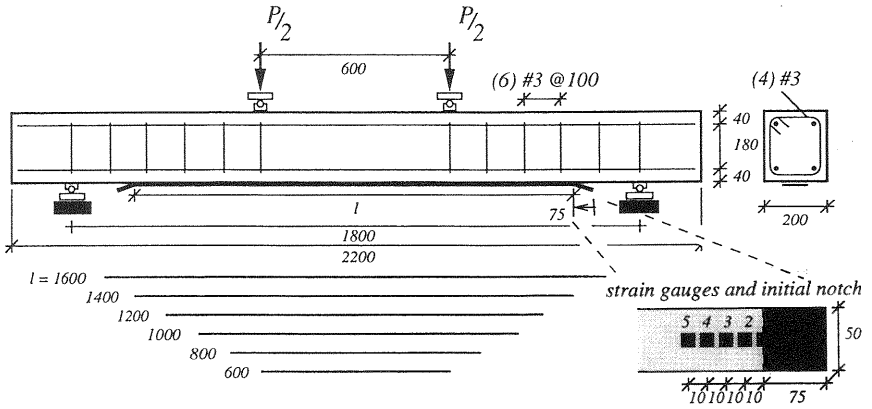

Fig. 2. Specialized delamination test specimen (dimensions in *mm*)

3 Experimental Program

Specialized delamination beam specimens were developed and tested in an experimental program to study local delamination fracture processes.

3.1 Specimen

To isolate local delamination mechanisms from other failure processes, a four-point beam specimen was designed with over-reinforced shear capacity, as shown in Fig. 2. To reduce the influence of shear cracks on the delamination process, the beams were over-reinforced with closely spaced stirrups that increased the shear strength to 175% of the flexural capacity of the retrofitted system. Delamination was studied by propagation from the end of the laminate towards the center of the specimen. To simulate steady-state conditions, initial delamination cracks were introduced with a thin sheet of plastic placed between the adhesive and concrete as the beam was retrofitted.

Table 1. Properties of materials used in the experimental program

Material	Tensile strength [*MPa*]	Compressive strength [*MPa*]	Elastic modulus [*GPa*]
Concrete	2.8	20.5	25.4
Steel	418.0	-	210.0
Adhesive	24.8	-	2.7
CFRP laminate	2700.0	-	155.0

Table 2. Results of the experimental program

Laminated Length [m]	Delamination intiation [kN]	Ultimate Load [kN]	Calculated energy release rate [J/m^2]	Failure Mode
Unlaminated	-	48.2	-	Steel yield
0.6	27.8	52.3	62.3	Debonding
0.8	35.2	53.8	39.8	Debonding
1.0	31.1	62.1	36.3	Debonding
1.2	39.6	63.2	34.4	Debonding
1.4	60.0	90.6	35.9	Debonding
1.6	97.3	100.4	24.2	Debonding

3.2 Materials and Procedure

The internal reinforcement in the beam specimens consisted of two #3 (ϕ=9.5 *mm*) reinforcing bars for both tensile and compressive steel. The external reinforcement consisted of CFRP laminate sheets 1 *mm* × 50 *mm* containing a fiber volume fraction of 70% with an epoxy matrix. The adhesive used was a high-strength high-modulus epoxy paste specifically designed for bonding to concrete surfaces applied with an average thickness of 1 *mm*. Properties of the materials used are listed in Table 1. Various lengths of laminate were applied to the beams and allowed to cure for at least 24 hours. Ten strain gauges (five on each end) were applied to selected specimens at the anchorage zone, also illustrated in Fig. 2. The specimens were loaded in four point bending in load steps of 4.5 *kN* until system failure. Midspan deflections and strain gauge signals were monitored continuously. The anchorage zones were inspected for delamination initiation at each load level using a magnifying scope.

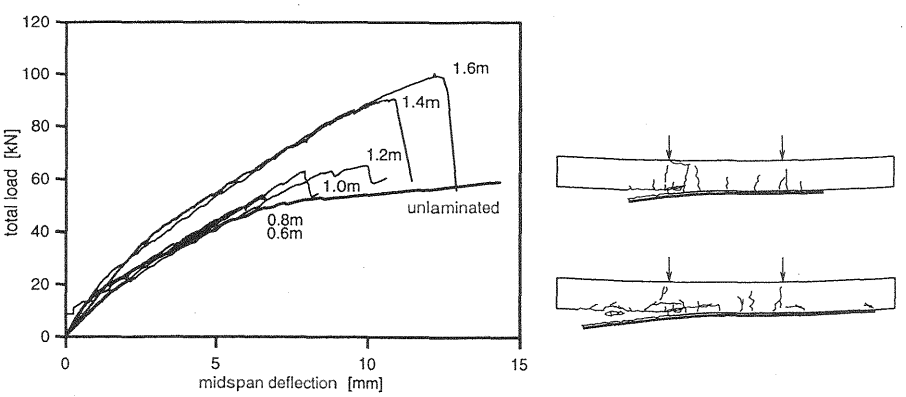

(a) Midspan deflection/load curves

(b) Typical crack patterns and failure modes

Fig. 3. Midspan deflection and cracking patterns for experimental program

3.3 Experimental Results

First, unretrofitted control beams were tested. The midspan deflection curves demonstrate traditional nonlinearities at cracking of the concrete and plasticity of the steel, as shown in Fig. 3(a). Typical cracking patterns are illustrated in Fig. 3(b), and it is shown that concrete cracking was largely limited to flexural cracks in the constant moment span. Then, laminated beams were tested; midspan deflection curves are also shown in Fig. 3(a), and typical cracking patterns are illustrated in Fig. 3(b). Ultimate loads from the testing program are presented in Table 2. The beams exhibited concrete cracking at levels higher than the unlaminated beams, with flexural cracking confined mostly to the constant moment span. Stiffnesses were observed to increase with the addition of the laminate. Strain gauge results indicated development of laminate stresses in the anchorage region, as illustrated with different loads in Fig. 4(a).

All retrofitted specimens failed through delamination in the concrete, leaving a thin layer of concrete substrate bonded to the delaminated FRP. Initial cracking in the concrete substrate at the delamination/anchorage zone was typically observed after flexural cracking, and before yielding of the steel or final delamination. These initial cracks were often accompanied by audible noises, and changes in stiffness were also observed in the midspan deflection curve. The strain gauge readings indicated that strains in the laminate reached their peaks at crack initiation, and decreased upon further loading, as shown for the beam with 1.4 *m* bonded length in Fig. 4(b). This indicates the initiation of the delamination process (at 60 *kN* for the beam shown), even though in this case the beam continued to resist more load. Upon additional loading the initial crack continued to widen until the ultimate load of the beam was

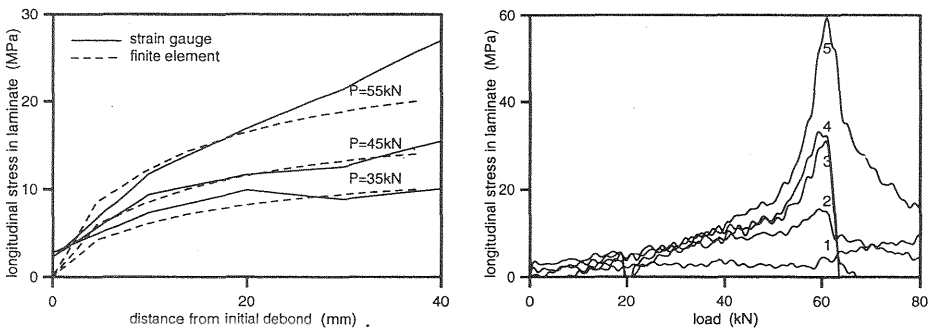

(a) Development of laminate stresses in anchorage zone

(b) Laminate stresses with load history

Fig. 4. Results from the strain gauges on the beam with 1.4 m bonded length

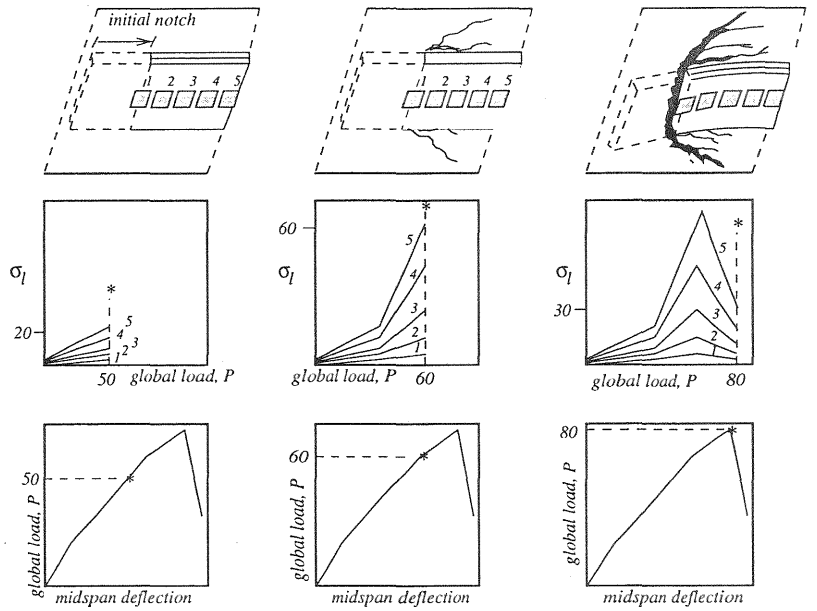

Fig. 5. Delamination process zone development with idealizations of Figures 4(b) and 3(a) for the 1.4 m laminate length beam

reached (at 90 *kN* for the beam shown), where unstable delamination occurred resulting in peeling of the laminate, adhesive, and a thin layer of concrete. This process is illustrated in Fig. 5 with idealizations of behavior demonstrated in Fig 4(b) and 3(a).

3.4 Effect of Bonded Length

From the results listed in Table 2, it is shown that loads at initiation of the delamination process and ultimate failure loads increased with longer laminate lengths. Beam stiffnesses were also found to increase, as shown in Fig. 3(a). Beams with longer laminate lengths demonstrated more brittle failure, with sudden delamination along the entire shear span. These longer laminates also had less delay between first signs of delamination and ultimate failure. Shorter laminate lengths were found to fail at lower loads with less brittleness. Delamination crack initiation was observed early, and there was a larger load delay between initiation and ultimate failure than with the longer laminates. The bonded laminate length was found to have significant influence on the load at which the delamination process is intiated. Causes of this process were further investigated in an analytical procedure.

4 Analytical Procedure

In the experimental procedure it was established that a delamination process zone develops at locations of stress concentrations in the concrete-adherent-laminate region before ultimate delamination and failure of the system. The development of this process and stress field information were further investigated in an analytical procedure incorporating a finite element model.

4.1 Finite Element Investigation

Numerical simulations of the initially notched delamination specimen were conducted using a nonlinear finite element method incorporating a smeared crack concrete material model. The beams strengthened with CFRP plates were symmetrically modeled with 18.75 *mm* square 8-node 2D plane strain elements and 3-node truss members for reinforcing steel. The mesh, shown in Fig. 6(a), is focused near the initial delamination notch, and perfect bond was assumed at the adhesive, CFRP, and concrete interfaces. The mechanical properties measured in the experimental procedure were used with the nonlinear material models. Concrete tensile softening was modeled through a bilinear curve, as illustrated in Fig. 6(b), and the reinforcing steel, epoxy, and CFRP materials were assumed to have bilinear plasticity. The beam was loaded through load steps of 1 *kN* until the mesh stiffness could no longer converge. Simulations of four laminate lengths were conducted. Strains in the FRP plate in the anchorage region are plotted in Figure 4(a). During the simulations, a crack band originating from the initial notch was observed. Failure was achieved through nonconvergence at a concrete node in the anchorage region for all simulations conducted. Nonconvergence was due to crack openings exceeding the ultimate tensile strain of the concrete; these loads are given in Table 3. The results of the finite element analyses indicated that delamination failures occur only when both the strength and ultimate strain of concrete are exceeded in the anchorage zone, suggesting that a

Table 3. Nonconvergence results from the finite element investigation

Laminated length [*m*]	Nonconvergence load [*kN*]
0.6	30.0
0.9	34.0
1.2	50.0
1.5	64.0

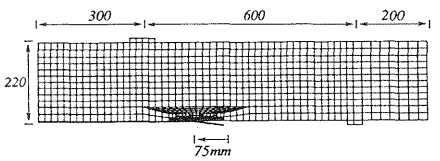

(a) Refined finite element mesh

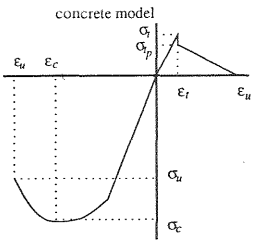

(b) Concrete model

Fig. 6. Models used in the finite element investigation

fracture energy approach may be applicable as a criteria for the delamination failures studied.

4.2 Fracture Energy Criterion

The Griffith energy criteria for fracture states that crack growth can occur if the energy required to form additional crack length can be delivered by the system. This condition for crack growth is

$$\frac{dW}{da} = \frac{d}{da}(F - U) \tag{1}$$

where U is the elastic energy contained in the system, F is the work provided by external forces, and dW/da is the crack resistance. The elastic energy contained in a beam structure under bending and shear forces M and V can be estimated by integrating the normal and shear stresses over the cross sectional area. The beams tested in this investigation can be discretized into five divisions of similar cross sections and applied loading, as illustrated in Fig. 7. The delamination process in the tested beams is simulated by advancing the delamination location of a by da, and transforming the laminated section (EI_l and GA_l) to unlaminated section (EI_u and GA_u) where EI_i and GA_i are the discrete section bending and shearing stiffnesses dependent on the integral load level, respectively

$$\frac{dW}{da} = \frac{M_a^2}{2b}\left(\frac{1}{EI_u} - \frac{1}{EI_l}\right) + \frac{V_a^2}{2b}\left(\frac{k_u}{GA_u} - \frac{k_l}{GA_l}\right) \tag{2}$$

where k_u and k_l are constants in the calculation of shearing stresses of the cross section and b is the width of the beam (Theillout, 1986). The stiffnesses can be estimated using conventional methods such as a strain

compatibility and force equilibrium (Plevris and Triantafillou, 1994) to find neutral axis depth fraction c of beam height h

$$c^2[h]+c[h\eta_s\rho'_s+2h\eta_s\rho_s+h\eta_l\rho_l]-2[d'\eta_s\rho'_s+d\eta_s\rho_s+h\eta_l\rho_l]=0 \quad (3)$$

where η_s and η_l are stiffness ratios of the reinforcing steel and laminate to the concrete and ρ_s, ρ'_s, and ρ_l are reinforcement ratios of the tensile steel, compressive steel, and laminate, respectively. Stiffnesses can be estimated for a given load by assuming that concrete cannot sustain tension over its rupture strength. The influence of the thin FRP laminate on the shear capacity of the beam is unclear (Jansze, 1997); in this analysis, the difference in the shear components in Equation (2) was neglected. Taking moments of areas about the neutral axis ch, the stiffness EI is estimated by

$$EI=\frac{E_c b_c (ch)^3}{3}+A_s E_s (d_s-ch)^2+E_{FRP}A_{FRP}h^2(1-c)^2 \quad (4)$$

where E_i and G_i are the elastic and shear modulus of material i (=c for concrete, s for steel, and FRP for FRP laminate), b_c is the width of the concrete, A_s and A_{FRP} are the areas of the reinforcing steel and laminate, and d_s is the depth to the reinforcing steel.

Energy release rates were calculated using this analytical procedure and the results from the experimental program, as shown in Table 2. The critical energy release rates are shown to be similar and independent of laminate length. Differences in data are found in the shortest (0.6 m) and longest (1.6 m) laminate lengths tested; these differences are attributed to influences such as steel yielding and possible shear cracking respectively. The procedure was repeated in reverse, using the fracture energy of the concrete as the delamination criteria dW/da. Because the moment of inertia calculations are dependent on the applied loading, an incremental load loop was repeated using increasing load levels in Equation (4) until the applied moment and moments of inertia exceeded the concrete's

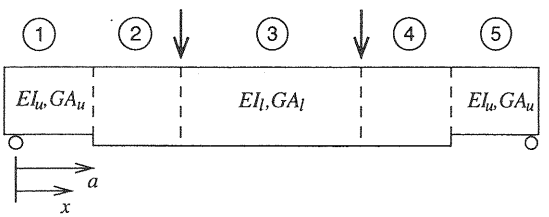

Fig. 7. Idealization of laboratory specimen into discrete cross sections

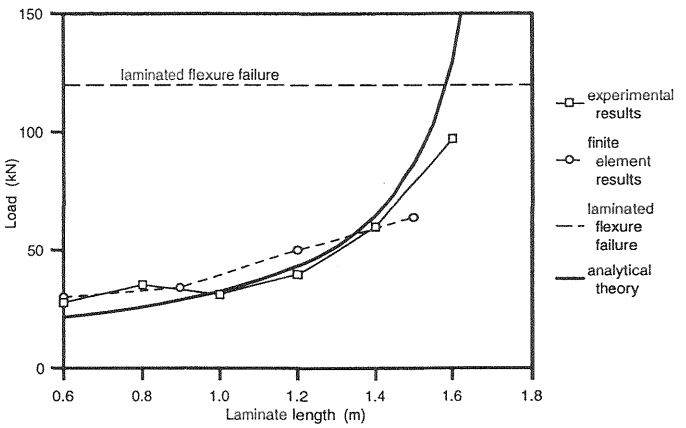

Fig. 8. Delamination loads predicted analytically with experimental and finite element results

fracture energy through Equation (2). These calculated delamination loads are plotted in Fig. 8 with the results from the experimental program and finite element investigation. It is shown that this procedure approximates the delamination load trend reasonably well, and that the load increases with longer laminate lengths. This trend indicates a critical laminate length where the tensile strength of the laminate will be exceeded before delamination occurs.

5 Conclusion

In this paper, delamination of reinforced concrete beams retrofitted with fiber-reinforced plastic laminates is investigated. Local failure processes were studied through laboratory tests on initially notched beam specimens retrofitted with various lengths of CFRP laminate. The beams were observed to fail through delamination at ultimate loads that increased with longer laminate lengths. This mechanism was further investigated using a finite element model, and failure was shown to occur only after both ultimate stresses and strains of the concrete were exceeded in the process zone. An analytical technique was used to calculate energy release rates of the experimental beams. The procedure was then conducted in reverse using the fracture energy of the concrete as the failure criteria, and the predicted loads were shown to match the experimental results. It is concluded that the critical energy release rate of the concrete may be applicable as a criterion for local delamination.

Acknowledgment

This work is supported by the National Science Foundation. The cognizant official is Dr. Ken Chong.

References

Anandarajah, A. and Vardy, A. E. (1985). A theoretical investigation of the failure of open sandwich beam due to interfacial shear fracture. **The Structural Engineer**, 63B(3), 85-92.

Buyukozturk, O. and Hearing, B. (1998) Failure behavior of precracked concrete beams retrofitted with FRP. *to appear in* **ASCE Journal of Composites in Construction**.

Hankers, C. (1997) **Zum verbundtragverhalten laschencerstarkter benbauteile unter night vorviegen ruhender beanspruchung**. Technical report, Beuth Verlag GmbH, Berlin.

Jansze, W. (1997) **Strengthening of Reinforced Concrete Members in Bending by Externally Bonded Steel Plates**. PhD thesis, Delft University of Technology.

Karbhari, V. M., Engineer, M., and Eckel II, D. A. (1997) On the durability of composite rehabilitation schemes for concrete: Use of a peel test. **Journal of Material Science**, 32(1), 147-156.

Meier, U. (1992) Carbon fiber-reinforced polymers: Model materials in bridge engineering. **Structural Engineering International**, 2(1), 7-12.

Plevris, N. and Triantafillou, T. (1994) Time-dependent behavior of RC members strengthened with FRP laminates. **ASCE Journal of Structural Engineering**, 120(3), 1016-1041.

Taljsten, B. (1997) Strengthening of beams by plate bonding technique. **ASCE Journal of Materials in Civil Engineering**, 9(4), 206-213.

Theillout, J. N. (1986) Repair and strengthening of bridges by means of bonded plates, in **Adhesion Between Polymers and Concrete** (ed. Sasse, H. R.), 601-621.